Antiviral Research 167 (2019) 83–88

Contents lists available at ScienceDirect

Antiviral Research

journal homepage: www.elsevier.com/locate/antiviral

A potential long-acting bictegravir loaded nano-drug delivery system for HIV-1 infection: A proof-of-concept study

Subhra Mandal[a], Pavan Kumar Prathipati[a], Michael Belshan[b], Christopher J. Destache[a,c,*]

[a] School of Pharmacy & Health Professions, Creighton University, Omaha, NE 68178, USA
[b] Department of Medical Microbiology & Immunology, Creighton University School of Medicine, Creighton University, Omaha, NE, USA
[c] School of Medicine, Division of Infectious Diseases, Creighton University, Omaha, NE 68178, USA

ARTICLE INFO

Keywords:
Antiretroviral therapy
Nanoparticles
Bictegravir
HIV-1 prophylaxis

ABSTRACT

Bictegravir (BIC), a newly FDA-approved integrase strand transfer inhibitor (INSTI), as a single tablet regimen has proven efficacious in treating HIV-1 and SIV viruses, with reduced resistance. BIC clinical trials have not investigated its prophylaxis potency. This study investigates the HIV prevention potency of a novel long-acting BIC nano-formulation aimed to improve adherence. Poly (lactic-co-glycolic acid) loaded BIC nanoparticles (BIC NPs) were formulated using an oil-in-water emulsion methodology. BIC NPs were < 200 nm in size, with 47.9 ± 6.9% encapsulation efficiency. A novel, sensitive and high throughput LC-MS/MS method was used to estimate intracellular pharmacokinetics (PK) of BIC NPs and compared to BIC solution demonstrated prolonged intracellular BIC retention. BIC NPs safety was assessed based on cytotoxicity. Further, *in-vitro* prevention study of BIC NPs vs BIC solution was assessed against HIV-1_{NLX} and HIV-1_{ADA} on TZM-bl cell line and PBMCs, respectively. BIC nanoencapsulation demonstrated elevated cellular cytotoxicity concentration (CC_{50}: 2.25 μM (BIC solution) to 820.4 μM (BIC NPs)] and lowers HIV-1 inhibitory concentration [EC_{50}: 0.604 μM (BIC solution) to 0.0038 μM (BIC NPs)) thereby improving selectivity index (SI) from 3.7 (BIC solution) to 215,789 (BIC NP) for TZM-bl cells. Comparable results in PBMCs were obtained where BIC NPs improved SI from 0.29 (BIC solution) to 523.33 (BIC NPs). This demonstrates long-acting BIC nano-formulation with sustained drug-release potency, improved BIC cytotoxicity and enhanced HIV-1 protection compared to BIC in solution.

1. Introduction

Bictegravir (BIC) is a new integrase strand transfer inhibitor (INSTI) approved by Food and Drug Administration (FDA) in 2018 (Gilead Sciences, 2018). It has shown potency against resistant and sensitive HIV-1 and SIV viruses (Gallant et al., 2017a, 2017b; Hassounah et al., 2017; Sax et al., 2017a, 2017b). In all reported Phase II-III trials, BIC has been formulated as a single daily tablet regimen (STR) along with emtricitabine (FTC) and tenofovir alafenamide (TAF). Phase III clinical trials have reported > 90% efficacy. BIC-based regimens were well tolerated with < 2% of patients discontinuing therapy due to adverse events (Gallant et al., 2017a; Sax et al., 2017b).

To improve patient's adherence to a regimen, the search for long-acting (LA) antiretroviral (ARV) drugs is presently one of the major goals of the HIV research agenda. Various long-acting injectable small molecule ARV agents are already in clinical trials (Spreen et al., 2013). Our research goal is to introduce long-action to conventional ARVs by fabricating single or multiple ARV (combination ARVs, cARVs) in polymeric nanoformulations as a long-acting parenteral drug delivery system for HIV treatment and prevention (Mandal et al., 2017b, 2017c; Prathipati et al., 2017; Shibata et al., 2013). Our long-acting FTC NPs (Mandal et al., 2017a), TAF + FTC NPs as well as TAF + elvitegravir (EVG) NPs were efficacious as prevention regimens (Mandal et al., 2017b, 2017c; Prathipati et al., 2017; Shibata et al., 2013), and TAF + FTC + EVG NPs demonstrated efficacy as chronic HIV treatment (Mandal et al., 2018) in humanized mice.

In the current study, BIC was nano-formulated into a polymer with the potential for extended release upon parenteral delivery. This report describes preliminary *in vitro* studies reflects the incorporation of BIC into a nanoformulation for extended release with improved therapeutic selectivity.

* Corresponding author. Creighton University, 2500 California Plaza, Omaha, NE 68178, USA.
E-mail address: destache@creighton.edu (C.J. Destache).

https://doi.org/10.1016/j.antiviral.2019.04.007
Received 16 October 2018; Received in revised form 9 January 2019; Accepted 10 April 2019
Available online 13 April 2019
0166-3542/

Abbreviations

BIC	bictegravir
INSTI	integrase strand transfer inhibitor
STR	single daily tablet regimen
FTC	emtricitabine
DTG	dolutegravir
LA	long-acting
ARV	antiretroviral
cARV	combination ARV
EVG	elvitegravir
TAF	tenofovir alafenamide
NPs	nanoparticles
PLGA	poly lactic-co-glycolic acid
DCM	dichloromethane
PBS	phosphate-buffered saline
ACN	acetonitrile
AcOH	acetic acid
EDTA	ethylenediaminetetraacetic acid
DMSO	dimethyl sulfoxide
%EE	percentage encapsulation efficiency
SEM	Scanning Electronic Microscope
DLS	Dynamic light scattering
PDI	polydispersity index
HPLC	high pressure liquid chromatography
LC-MS/MS	liquid chromatography-tandem mass spectrometry
MWCO	molecular weight cut-off
AUC	area under the curve
CC_{50}	50% cytotoxicity concentration
EC_{50}	50% effective concentration
SI	selectivity index

2. Materials and methods

2.1. Materials

BIC (purity: > 98%) was purchased from MuseChem, (San Gabriel, CA, USA). Whereas, poly lactic-co-glycolic acid (PLGA, with lactide:glycolide at 75:25 ratio; Mw 4000–15,000), dichloromethane (DCM), acetic acid (AcOH), ethylenediaminetetraacetic acid (EDTA), interleukin-2 (IL-2), phosphate buffered saline (PBS) were obtained from Sigma-Aldrich (St. Louis, MO, USA). DTG (purity: > 98%) was purchased from Biochempartner Co., Ltd., China. Acetonitrile (ACN) and methanol were purchased from Fisher Chemicals (Fair Lawn, NJ, USA), whereas Pluronic F127 (PF-127) was from D-BASF (Edinburgh, UK). Dimethyl sulfoxide (DMSO) and formic acid were purchased from ThermoScientific (Rockford, IL, USA). High glucose Dulbecco's Modified Eagles Medium (HiDMEM) with L-Glutamine, Roswell Park Memorial Institute (RPMI) 1640 medium, fetal bovine serum (FBS) trypsin-EDTA solution 10S and antibiotic-antimycotic solution 100× (AA) were purchased from Corning (Manassas, VA, USA). All the reagents were used without any further purification.

2.2. Cell line

TZM-bl cells were obtained from NIH AIDS reagent program (Kappes and Wu, 2018; Kappes et al., 2015). Peripheral blood mononuclear cells (PBMCs) were obtained from commercial vendor (AllCells Inc. Alameda, CA). TZM-bl cells were maintained in complete HiDMEM medium (supplemented with 10% FBS and 1XAA solution). PBMCs were maintained in complete RPMI-1640 medium (supplemented with 10% FBS, IL-2 100U/mL and 1xAA) under 5% CO_2 at 37 °C and > 80% humidity.

2.3. HIV strains

HIV-1_{NLX} and HIV-1_{ADA} viruses were obtained from the NIH AIDS reagent Program (Malcolm, 2017). Further, the HIV-1_{NLX} and HIV-1_{ADA} viruses were expressed and purified by following previously described protocol (Cartier et al., 2003). Tissue Culture Infective Dose for 50% of strains ($TCID_{50}$/mL) was found to be 10 µL and 20 µL for HIV-1_{NLX} and HIV-1_{ADA} viruses (representing 1.5×10^6 and 1.58×10^5 viral particles/µL, respectively).

2.4. BIC NP formulation and characterization

BIC loaded NPs (BIC NPs) were formulated using previously reported oil-in-water (o-w) emulsion method with some modifications (Destache et al., 2016; Mandal et al., 2017c; Prathipati et al., 2017). Briefly, the 5 mL DCM (organic phase) containing PLGA, PF-127 (stabilizer) and BIC at 10:10:2 (w:w:w), respectively, was added dropwise to 20 mL of 1% PVA solution (aqueous phase), under high speed continuous stirring condition. The o-w emulsion thus obtained was probe-sonicated (% Amplitude: 90; cycle: 0.9; UP100H ultrasonic processor (100 W, 30 kHz), Mount Holly, NJ, USA) for 5 min on ice. The organic phase was eliminated by overnight (O/N) evaporation. BIC NPs obtained were freeze-dried by Millrock LD85 lyophilizer (Kingston, NY, USA) and stored at 4 °C until used. All the methodology was carried out in a biosafety cabinet to maintain sterility.

For physicochemical properties determination, an appropriate amount of freeze-dried BIC NP was dispersed in ultrapure water at room temperature (RT). Dynamic light scattering (DLS), polydispersity index (PDI; a measure of the NP size heterogeneity in the given population) were performed to determine the size and size-distribution pattern of BIC NP, whereas surface charge was determined by zeta potential analysis using the ZetaPlus Zeta Potential Analyzer (Brookhaven Instruments Corporation, Holtsville, NY, USA).

The percentage encapsulation efficiency (%EE) was evaluated by high performance liquid chromatography (HPLC) analysis (Shimadzu, Kyoto, Japan). Briefly, BIC (absorbance maximum at 260 nm, retention time 6.5 min) loading concentrations in 1 mg of BIC NPs dissolved in DMSO was verified based on the standard curve determined by HPLC analysis (details in the HPLC section below) (Mandal et al., 2018). The %EE was calculated by the following equation:

$$\%EE = \frac{(Amount\ of\ drug\ loaded\ in\ the\ NP)}{(Amount\ of\ drug\ used)} \times 100 \quad (1)$$

Three different batches of BIC NPs were produced to evaluate the reproducibility of the formulation. Data were reported as mean ± standard error of mean (SE).

The morphology and tomography of BIC NPs were determined by Scanning Electronic Microscope (SEM) imaging following our previously described method (Mandal et al., 2017a). Briefly, BIC NPs were filtered through ~50 nm pore size Whatman® Nuclepore Track-Etch Membrane (Sigma-Aldrich, St. Louis, MO, USA), air dried on SEM stub, sputter coated and imaged with a Hitachi S-4700 Field-emission SEM instrument (Hitachi, NY, USA).

2.5. BIC release profile in simulated endosomal pH

To evaluate BIC sustained release from the nano-formulation, 5 mg/mL BIC NP (i.e. 50 µg BIC entrapped) dissociated in simulated endosomal solution (20 mM citrate buffer, pH 5.5), as described previously (Prathipati et al., 2018). Briefly, at specific times (1 and 16 h, 1, 4, 7, and 14 days), 200 µL supernatant was collected after brief vortexing. The supernatant was filtered through spin-filter (100 K MWCO,

PES filter; ThermoScientific, Rockford, IL, USA). For BIC standards the same procedure was followed. The BIC standards and amount of BIC release were evaluated by HPLC following methodology described below in HPLC chromatography section. The % BIC released at respective time-point was calculated by following equations

$$\%\ BIC\ released = \frac{(BIC\ concentration\ in\ sup_t)}{(BIC\ in\ BIC\ NP_t)} \times 100 \quad (2)$$

Where, 'sup_t', 'NP_t' represents 'supernatant collection at respective time', and 'BIC still entrapped at respective time'.

To maintain sink condition, at each time-point equal volume was collected, and spun down by centrifugation (14000×*g* for 5 min at 4 °C) for supernatant collection. To determine the amount of BIC released from BIC NP at respective time and volume, the BIC concentration was determined by HPLC analysis as described in the HPLC chromatography method section and % BIC release was calculated by equation (2). The result represents mean ± SE of 3 independent sets of experiments (performed in triplicate).

2.6. HPLC chromatography method

The BIC % EE in BIC NPs and the BIC release profile in simulated endosomal pH was estimated by HPLC chromatography. Briefly, the Phenomenex® C-18 (150 × 4.6 mm, particle size 5 µm) column (Torrance, CA, USA) was used for chromatographic separation, using isocratic elution process with the mobile phase (0.5% AcOH:ACN ratio at 45:55, v/v). The column was maintained at the flow rate of 0.5 mL/min; temperature: 25 °C; and BIC was detected by UV-detector at 260 nm (retention time 6.5 min). Quantification was based on the area under the curve (AUC) analysis. The amount of BIC in the unknown samples was analyzed based on the BIC standard concentrations ranging between 0.0019 and 0.5 mg/mL (a linear correlation, $r^2 \geq 0.99$). The HPLC instrument (Shimadzu Scientific Instruments, Columbia, MD, USA) equipped with SIL-20AC auto-sampler, LC-20AB pumps, and SPD-20A UV/Visible detector. The inter-day and intra-day variability of the instrument was < 10%.

2.7. Cytotoxicity assay

The comparative *in-vitro* cytotoxicity between BIC NP and BIC solution was evaluated on TZM-bl cells and PBMCs using CellTiter-Glo® luminescent assay, as described previously (Mandal et al., 2017a). Briefly, triplicate TZM-bl cells (10^4 cells/well) were treated with BIC NP and BIC solution respectively, at different concentrations (44.5, 22.25, 2.225, 0.2225, and 0.02225 µM) for 96 h in triplicate. The 5% DMSO treated cells were considered as the positive control and treatment equal-volume 1×PBS was added to untreated cells was considered the negative control. Similar procedures as described above were followed to treat triplicate PBMCs (10^5 cells/well). The CellTiter-Glo® luminescent cell viability assay kit (Promega, Madison, WI, USA) was used to determine cytotoxicity following manufacturer protocol. The luminescence was read on a Synergy II multi-mode reader with Gen5TM software (BioTek, Winooski, VT, USA). The percentage cytotoxicity values were calculated based on % viability normalized against the untreated negative control group. The experiments were carried out for three independent times and the results are presented as mean ± SE.

2.8. Intracellular PK studies

For *in vitro* PK and time-dependent BIC uptake/retention studies, TZM-bl cells (10^4 cells/well) were seeded in Nunc 96-well plates; the cells were treated at 2.225 µM of BIC as BIC NPs or in solution, respectively. For time-dependent uptake studies, cells were treated respectively for 1, 4, 8, 16 and 24 h (before wash). At specific time, treated and control cells were washed thrice with 1×PBS and after wash the cell number per well were re-counted (considered for BIC intracellular concentration determination). Whereas for retention studies, after 24 h of treatment, the treatment was washed-off by warm 1 × PBS wash (thrice) and cells were maintained in fresh complete HiDMEM medium until harvesting (i.e. 1, 4, 8, 16, 24, and 96 h after wash, corresponding to 25, 28, 32, 40, 48, and 120 h, respectively). All the plates were air dried in biosafety cabinet and stored at −80 °C until analysis. The samples were further processed as per our standardized reported method (Prathipati et al., 2018) and described in LC-MS/MS section below.

2.9. LC-MS/MS method

The adhered dried cells were detached from the surface of 96-well plate by adding 30 µL of 0.5% EDTA solution and vortexed for 30 min. Later, cells were lysed with 70 µL methanol and vortex mixed for 30 min. The samples were thoroughly mixed, transferred to micro centrifuge tubes and centrifuged at 14,000 rpm for 5 min at 4 °C. A 50 µL clear supernatant was added to 200 µL ACN containing 100 ng/mL internal standard, DTG. Samples were vortexed, centrifuged and transferred to autosampler vials for analysis using LC-MS/MS (Prathipati et al., 2018).

AB Sciex 5500 Q Trap mass spectrometer (Applied Biosystems, Foster City, CA, USA) operated in positive mode with Exion liquid chromatograph (Applied Biosystems, Foster City, CA, USA) as front end was used for analysis. An isocratic mobile phase comprising 80: 20 v/v ACN and water with 0.1% formic acid at a flow rate of 0.25 mL/min and Phenomenex Kinetex EVO C18 column (50 × 3.0 mm, 5 µm) were used. BIC and DTG mass transitions were 450.1 → 289.1 and 420.1 → 277.1, respectively. A two-microliter sample was injected into LC-MS/MS equipment. The LC-MS/MS assay for BIC detection was validated in human plasma at the range 1–10,000 ng/mL.

2.10. In vitro protection study

The *in vitro* short-term HIV protection (24 h pre-treatment) against HIV-1_{NLX} and HIV-1_{ADA} was performed on TZM-bl, a HIV-1 reporter cell line and on PBMCs following previously reported standardized methodology (Mandal et al., 2017a, 2017c). Briefly, TZM-bl (10^4 cells/well) and PBMCs (10^5 cells/well) were treated with different concentrations of BIC (44.5, 22.25, 2.225, 0.2225, 0.02225, 0.00223, 0.00022 µM) either as BIC NP or BIC solution. As negative and positive control respectively, untreated/uninfected cells and untreated/infected cells were used. After 24 h of treatment, the TZM-bl cells were inoculated with HIV-1_{NLX} virus (MOI: 0.1) and PBMCs were inoculated with HIV-1_{ADA} (MOI: 1) for 16 h. Subsequently, the inoculated and control cells were washed thrice with warm 1 × PBS. TZM-bl cells and PBMCs were maintained in respective fresh complete HiDMEM medium for 4 days. HIV-1 infectivity of TZM-bl cells and PBMCs were determined by Steady-Glo® luciferase assay company defined protocol (Promega, Madison, WI, USA) and p24 Antigen ELISA kit (ZeptoMetrix, Buffalo, NY), respectively following company protocol. For Steady-Glo luciferase assay, luminescence intensity was read as relative luminescence units (RLU) and p24 ELSIA was read as optical density at 450 nm on the Synergy HT Multi-Mode Microplate Reader (BioTeck, Winooski, USA). The % HIV-1 infection was calculated by following equation (4):

$$\%\ \text{HIV protection/inhibition} = \frac{(L_{untreated/infected} - L_{treated/infected})}{L_{untreated/infected}} \times 100 \quad (3)$$

Where, '$L_{untreated/infected}$' represents the luminescence intensity or optical density respectively of untreated + virus infected TZM-bl cells or PBMCs. Similarly, '$L_{treated/infected}$' represents BIC treated (as BIC NP or BIC solution) + virus infected TZM-bl cells or PBMCs. As a negative control, untreated + uninfected cells were used. Three independent

experiments were performed with three different BIC NP batches (each performed in triplicate) for TZM-bl cells and from three different PBMC donors. Finally, the selectivity index (SI), was evaluated by following equation

$$SI = \frac{CC_{50}}{EC_{50}} \quad (4)$$

Where, 'CC_{50}' and 'EC_{50}' represents respectively, 50% cytotoxic concentration and 50% effective concentration.

2.11. Statistical analysis

All experimental results are presented as mean ± SE of the obtained data from three independent experiments. The CC_{50} value was determined by non-regression curve fitting based on log (BIC) vs. normalized luminescent (four parameter logistic fits) cytotoxicity response curves. Whereas, the EC_{50} was analyzed based on [BIC] vs. normalized TZM-bl luminescence or PBMC optical density (four parameter logistic fits) curves. Both CC_{50} and EC_{50} were determined using GraphPad Prism 7 software (La Jolla, CA, USA). Significant differences among treated (BIC NP and BIC in solution) and control groups were determined at $p \leq 0.05$.

3. Results

3.1. BIC NPs characterization

BIC, a highly hydrophobic drug was encapsulated in the PLGA NPs using o-w emulsion solvent evaporation method. The physiochemical characteristics of BIC NPs are summarized in Table 1. The BIC NP size was 189.2 ± 3.2 nm diameter with a narrow size distribution window (PDI < 0.2) and low negative surface charge (−24.3 ± 3.9 mV). The SEM image reveals the BIC NPs obtained were uniform and smooth spherical surface (Fig. 1). The encapsulation efficiency of BIC was estimated to be 47.9 ± 6.9% (Table 1).

3.2. BIC release kinetics at endosomal pH

To assess the BIC release profile from BIC NP at the endosomal subunit of cell, we studied BIC release kinetics from NP in simulated endosomal pH (pH = 5.5) (Fig. 2). The result demonstrated ~45% BIC from BIC NP were released within 1 h. After initial release, BIC tends to release relatively constantly with effective time constant (t_{eff}) of 15.02 h (rate constant, $K = 0.066\ h^{-1}$) until 70.0% release, as the plateau phase is reached. By the end of the experiments (14 days) the NP released ~72% of its total BIC content. The one phase decay analysis estimates the release half-life of 10.41 h.

3.3. Intracellular PK study

The intracellular uptake and retention kinetics of BIC as NP and solution were determined from obtained LC-MS/MS data analysis by using Phoenix WinNonlin 8.0 software. The intracellular BIC NP concentration maximum (C_{max}) and area under the time-concentration curve (AUC_{all}) was found to be 2.4 and 3.1 times higher for BIC NP treatment compared to BIC solution (Table 2). It is apparent from C_{max} and AUC_{all}, that BIC nano-encapsulation promotes BIC uptake and prolongs its intracellular retention. Additionally, BIC nanoformulation demonstrates slower clearance rate than free drug in solution.

Moreover, the BIC uptake kinetics demonstrates BIC NP enhances BIC uptake compared to BIC solution (Supplementary Fig. 1). Therefore, these study results demonstrate overall NP formulation enhanced the PK properties of BIC.

3.4. In vitro cytotoxicity

Encapsulation of BIC in NPs provides BIC a totally new physiochemical entity, therefore proper evaluation of BIC NP cytotoxicity prior to determining functionality is a mandatory step. TZM-bl are a modified HeLa cell line that mimic the functionally of endothelial cells (Kappes et al., 2015). These cells would be the first cell type that BIC nano-formulation will encounter upon ARV administration such as intravaginal, intramuscular or subcutaneous (subQ) administration. The cytotoxicity study in TZM-bl cells demonstrated CC_{50} values for BIC solution (2.25 ± 1.46 μM) and significantly enhanced by nano-encapsulation (BIC NPs 820.4 ± 2.27 μM) (Table 3). PBMC cytotoxicity assessment was also elevated 4.6 times (15.7 ± 1.33 μM) by BIC nano-encapsulation (Table 3).

3.5. In-vitro protection studies

The ARV property of BIC NPs compared to BIC solution was evaluated using a short-term 4-day protection study in TZM-bl cells and PBMCs after HIV_{NLX} and HIV_{ADA} infection. The EC_{50} from TZM-bl cells was estimated to be approximately 0.0038 μM for BIC NPs, compared to 0.604 μM for BIC in solution. The EC_{50} for BIC NPs from PBMCs averaged 0.076 ± 0.45 μM compared to 2.33 ± 2.15 μM for BIC solution. Therefore, BIC NPs enhances protection efficiency by ~159 times compared to BIC in solution for TZM-bl cells and 30 times for PBMCs (Table 3).

Finally, BIC nano-encapsulation demonstrated significant elevation in SI for both TZM-bl cells and PBMCs, calculated to be 215,789 and 523.33, respectively whereas the SI value for BIC in solution was estimated to be 3.7 and 1.5 (Table 3). BIC NP encapsulation increases significantly the therapeutic selectivity.

4. Discussion

All the above studies support the long-acting potency of nanoencapsulated BIC for HIV protection, with the overall goal to reduce the daily dosing to monthly and thus improve adherence. Compared to other marketed INSTIs including raltegravir, elvitegravir and dolutegravir administered once-daily, BIC displays improved PK and patient tolerability. BIC additionally has a high barrier for HIV-1 resistance (Tsiang et al., 2016). As nanotechnology induces long-acting potency to ARVs, besides polymeric nanoformulation, wet milling and solid lipid NPs are also being evaluated (Freeling et al., 2015; Spreen et al., 2013). Both formulations are in trials in animal models and humans. However, the physiochemical characteristics of this BIC NP formulation demonstrates small size (< 200 nm), low negative surface charge, and smooth spherical shape (Fig. 1) suggesting that BIC NPs could avoid fine capillary damage and blockage (Bose et al., 2014; Shao et al., 2015; Zhang and Lu, 2014). Additionally, the encapsulation of BIC (very hydrophobic drug) in PLGA as BIC NP, enhances BIC solubility compared to the solubility of BIC powder in aqueous medium (Drugbank, 2016).

The endosomal BIC release results (Fig. 2) are consistent with typical biphasic drug-release characteristics of PLGA nano-formulations (Makadia and Siegel, 2011). Therefore, the simulated endosomal release study suggests that upon endosomal uptake, 45% of the BIC is released due to initial burst, which contributes to the preliminary effective concentration in the cell to inhibit HIV integrase activity and

Table 1
BIC NP physicochemical characteristics.

Size (nm)	PDI	Surface charge (mV)	% EE
189.2 ± 3.2	0.142 ± 0.014	−24.3 ± 3.9	47.9 ± 6.9

Data represents as mean ± standard error of means (SE), n = 3; PDI = Polydispersity index; % EE = percentage encapsulation efficacy.

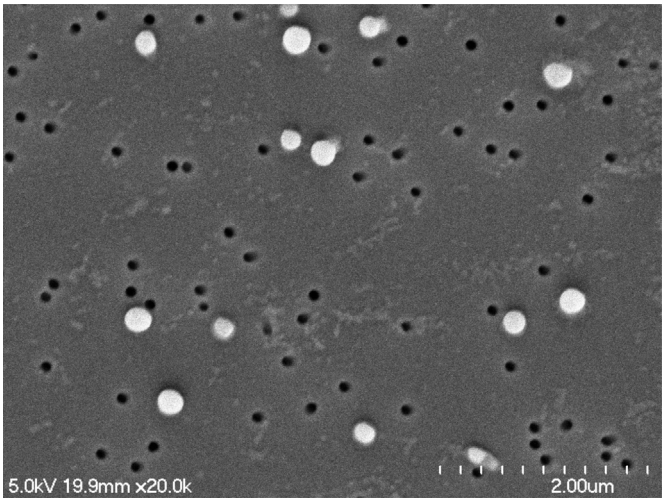

Fig. 1. SEM image evaluating morphological characteristic of BIC NP. The NP appear spherical in shape and average < 200 nm in diameter.

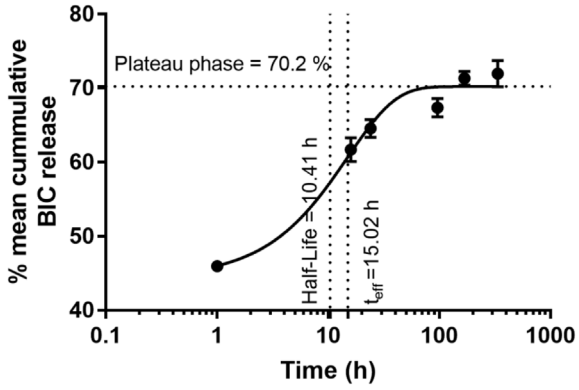

Fig. 2. BIC release kinetics from BIC NP in simulated endosomal fluid (pH 5.5). One-phase decay non-linear regression curve fitting equation was used for graph fitting and to analyze the half-life, effective release constant ($t_{eff.}$) and plateau release phase. The BIC release rate constant, K, was estimated to be 0.066 h^{-1}. Each data point represents mean ± SD values of three independent batches study (n = 3).

block viral DNA integration. Therefore, BIC controlled release from the polymeric NPs in the endosome and long *in vitro* retention together would prolong BIC functionality/effectiveness and introduce the long-acting characteristics to BIC potency.

Even though BIC has shown comparable potency to other INSTI *in vitro*, BIC was found to significantly more cytotoxic than DTG (Tsiang et al., 2016). The reported CC_{50} of BIC was lower compared to DTG averaging 7.3 μM vs 30.2 μM in a variety of cell lines, primary T-lymphocytes, macrophages, resting and activated peripheral blood mononuclear cells (PBMCs), respectively (Tsiang et al., 2016). Nanoencapsulation of BIC significantly elevates the CC_{50} > 350 times compared to BIC in solution in the TZM-bl cells and 4.6 times for PBMCs (Table 3). The enhanced CC_{50} value of BIC is due to encapsulation protecting BIC from direct contact with the cellular components contributing to reduced cellular efflux and probably reduced *in vivo* clearance. As PLGA polymer degrades, polymeric protection increases the tolerability index of BIC compared to BIC solution. This is important when considering a subcutaneous delivery modality to deliver BIC NPs. Moreover, recent phase III randomized clinical trials demonstrated good tolerability of BIC/TAF/FTC regimen (Gallant et al., 2017a; Sax et al., 2017a, 2017b). Thus our study demonstrates BIC nanoencapsulation may potentially improve the sustained-release properties and thus promote better adherence.

Table 3
In vitro safety and efficacy comparison of BIC NP versus BIC solution.

Cell type	Treatment Type	Cytotoxicity (CC_{50} (μM))	HIV inhibition (EC_{50} (μM))	Selectivity (SI)
TZM-bl cell line	BIC NP	820.4 ± 2.27	0.0038 ± 0.0023	215,789
	BIC solution	2.25 ± 1.46	0.604 ± 0.593	3.7
PBMCs	BIC NP	15.7 ± 1.33	0.076 ± 0.45	523.33
	BIC solution	3.4 ± 1.26	2.33 ± 2.15	1.5

The data represents means ± SE of three independent experiments or donors analyzed in triplicate, respectively. SI = CC_{50}/IC_{50}.

The *in vitro* HIV-1 prevention studies demonstrate that nano-encapsulation of BIC, in addition to lowering cytotoxicity also enhances anti-HIV potency and therefore, markedly extends the therapeutic selectivity compared to BIC in solution (Table 3). The endosomal release (Fig. 1) and PK (Supplementary Fig. 1) further suggests that BIC nanoencapsulation enhances BIC intracellular concentration and confirmed sustained BIC retention (Supplementary Fig. 1) and therefore could be a reason protection against HIV-1 infection at a low (nanomolar) concentration. Further, on average BIC elucidates ~215,789 and 523 times higher SI values compared to BIC solution on lymphoblastoid T-cell line and primary cell types.

In conclusion, the above results demonstrate that nano-formulation improves BIC therapeutic selectivity, intra-cellular delivery, retention, and induces controlled-release that potentially promotes sustained protection from HIV-1 challenge. Hence, this BIC nano-formulation could potentially be an efficient sustained-drug release delivery system that could potentially participate in both HIV-1 prevention and treatment strategies.

Conflicts of interest

No conflict of interest associated with any of the authors.

Acknowledgements

This work has been funded, in part, by the Creighton University School of Pharmacy & Allied Health Professions Wareham Research Fund (to S.M.). The sponsor did not have any influence in the study design or results and interpretation of the obtained data.

Appendix A. Supplementary data

Supplementary data to this article can be found online at https://doi.org/10.1016/j.antiviral.2019.04.007.

Table 2
In-vitro pharmacokinetic parameters of bictegravir (BIC) as NP and solution.

PK Parameter/10^6 cells	Unit	BIC NP	BIC Solution
C_{max}	pmole	888.54 ± 226.73	372.3 ± 137.54
AUC_{all}	h × pmole	31,654.77 ± 4186.15	10,053.24 ± 1187.96
Clearance	pmole/(h × pmole)	0.010	0.044

Data represents mean ± standard error of means (SE), n = 3; AUC_{all} = area under the plasma concentration-time curve (from 0-end of experiment).

References

Bose, T., Latawiec, D., Mondal, P.P., Mandal, S., 2014. Overview of nano-drugs characteristics for clinical application: the journey from the entry to the exit point. J. Nanoparticle Res. 16, 2527.

Cartier, C., Hemonnot, B., Gay, B., Bardy, M., Sanchiz, C., Devaux, C., Briant, L., 2003. Active cAMP-dependent protein kinase incorporated within highly purified HIV-1 particles is required for viral infectivity and interacts with viral capsid protein. J. Biol. Chem. 278, 35211–35219.

Destache, C.J., Mandal, S., Yuan, Z., Kang, G., Date, A.A., Lu, W., Shibata, A., Pham, R., Bruck, P., Rezich, M., Zhou, Y., Vivekanandan, R., Fletcher, C.V., Li, Q., 2016. Topical tenofovir disoproxil fumarate nanoparticles prevent HIV-1 vaginal transmission in a humanized mouse model. Antimicrob. Agents Chemother. 60, 3633–3639.

Drugbank, 2016. Bictegravir. Gilead Sciences, Foster city, CA, USA.

Freeling, J.P., Koehn, J., Shu, C., Sun, J., Ho, R.J., 2015. Anti-HIV drug-combination nanoparticles enhance plasma drug exposure duration as well as triple-drug combination levels in cells within lymph nodes and blood in primates. AIDS Res. Hum. Retrovir. 31, 107–114.

Gallant, J., Lazzarin, A., Mills, A., Orkin, C., Podzamczer, D., Tebas, P., Girard, P.M., Brar, I., Daar, E.S., Wohl, D., Rockstroh, J., Wei, X., Custodio, J., White, K., Martin, H., Cheng, A., Quirk, E., 2017a. Bictegravir, emtricitabine, and tenofovir alafenamide versus dolutegravir, abacavir, and lamivudine for initial treatment of HIV-1 infection (GS-US-380-1489): a double-blind, multicentre, phase 3, randomised controlled non-inferiority trial. Lancet 390, 2063–2072.

Gallant, J.E., Thompson, M., DeJesus, E., Voskuhl, G.W., Wei, X., Zhang, H., White, K., Cheng, A., Quirk, E., Martin, H., 2017b. Antiviral activity, safety, and pharmacokinetics of bictegravir as 10-day monotherapy in HIV-1-Infected adults. J. Acquir. Immune Defic. Syndr. 75, 61–66.

Gilead Sciences, I., 2018. Center for drug evaluation and research. Application number-210251Orig1s000. Trade Name: BIKTARVY tablets. In: Services, D.O.H.A.H. (Ed.), Food and Drug Administration. Silver Spring, MD, USA.

Hassounah, S.A., Alikhani, A., Oliveira, M., Bharaj, S., Ibanescu, R.I., Osman, N., Xu, H.T., Brenner, B.G., Mesplede, T., Wainberg, M.A., 2017. Antiviral activity of bictegravir and cabotegravir against integrase inhibitor-resistant SIVmac239 and HIV-1. Antimicrob. Agents Chemother. 61.

Kappes, J.C., Wu, X., 2018. TZM-bl Cells. NIH AIDS Reagent Program, Germantown, MD, USA.

Kappes, J.C., Wu, X., Inc, T., 2015. In: Program, N.A.R. (Ed.), TZM-bl Cells Data Sheet. Germantown, MD, USA.

Makadia, H.K., Siegel, S.J., 2011. Poly lactic-co-glycolic acid (PLGA) as biodegradable controlled drug delivery carrier. Polymers 3, 1377–1397.

Malcolm, M., 2017. HIV-1 NL4-3 Infectious Molecular Clone (pNL4-3). NIH AIDS Reagent Program, Germantown, MD, USA.

Mandal, S., Belshan, M., Holec, A., Zhou, Y., Destache, C.J., 2017a. An enhanced emtricitabine-loaded long-acting nanoformulation for prevention or treatment of HIV infection. Antimicrob. Agents Chemother. 61.

Mandal, S., Kang, G., Prathipati, P.K., Fan, W., Li, Q., Destache, C.J., 2018. Long-acting parenteral combination antiretroviral loaded nano-drug delivery system to treat chronic HIV-1 infection: a humanized mouse model study. Antivir. Res. 156, 85–91.

Mandal, S., Khandalavala, K., Pham, R., Bruck, P., Varghese, M., Kochvar, A., Monaco, A., Prathipati, K.P., Destache, C., Shibata, A., 2017b. Cellulose acetate phthalate and antiretroviral nanoparticle fabrications for HIV pre-exposure prophylaxis. Polymers 9.

Mandal, S., Prathipati, P.K., Kang, G., Zhou, Y., Yuan, Z., Fan, W., Li, Q., Destache, C.J., 2017c. Tenofovir alafenamide and elvitegravir loaded nanoparticles for long-acting prevention of HIV-1 vaginal transmission. AIDS 31, 469–476.

Prathipati, P.K., Mandal, S., Destache, C.J., 2018. Development and validation of LC–MS/MS method for quantification of bictegravir in human plasma and its application to an intracellular uptake study. Biomed. Chromatogr. 0, e4379.

Prathipati, P.K., Mandal, S., Pon, G., Vivekanandan, R., Destache, C.J., 2017. Pharmacokinetic and tissue distribution profile of long acting tenofovir alafenamide and elvitegravir loaded nanoparticles in humanized mice model. Pharm. Res. 34, 2749–2755.

Sax, P.E., DeJesus, E., Crofoot, G., Ward, D., Benson, P., Dretler, R., Mills, A., Brinson, C., Peloquin, J., Wei, X., White, K., Cheng, A., Martin, H., Quirk, E., 2017a. Bictegravir versus dolutegravir, each with emtricitabine and tenofovir alafenamide, for initial treatment of HIV-1 infection: a randomised, double-blind, phase 2 trial. Lancet HIV 4, e154–e160.

Sax, P.E., Pozniak, A., Montes, M.L., Koenig, E., DeJesus, E., Stellbrink, H.J., Antinori, A., Workowski, K., Slim, J., Reynes, J., Garner, W., Custodio, J., White, K., SenGupta, D., Cheng, A., Quirk, E., 2017b. Coformulated bictegravir, emtricitabine, and tenofovir alafenamide versus dolutegravir with emtricitabine and tenofovir alafenamide, for initial treatment of HIV-1 infection (GS-US-380-1490): a randomised, double-blind, multicentre, phase 3, non-inferiority trial. Lancet 390, 2073–2082.

Shao, X.R., Wei, X.Q., Song, X., Hao, L.Y., Cai, X.X., Zhang, Z.R., Peng, Q., Lin, Y.F., 2015. Independent effect of polymeric nanoparticle zeta potential/surface charge, on their cytotoxicity and affinity to cells. Cell Prolif 48, 465–474.

Shibata, A., McMullen, E., Pham, A., Belshan, M., Sanford, B., Zhou, Y., Goede, M., Date, A.A., Destache, C.J., 2013. Polymeric nanoparticles containing combination antiretroviral drugs for HIV type 1 treatment. AIDS Res. Hum. Retrovir. 29, 746–754.

Spreen, W.R., Margolis, D.A., Pottage Jr., J.C., 2013. Long-acting injectable antiretrovirals for HIV treatment and prevention. Curr. Opin. HIV AIDS 8, 565–571.

Tsiang, M., Jones, G.S., Goldsmith, J., Mulato, A., Hansen, D., Kan, E., Tsai, L., Bam, R.A., Stepan, G., Stray, K.M., Niedziela-Majka, A., Yant, S.R., Yu, H., Kukolj, G., Cihlar, T., Lazerwith, S.E., White, K.L., Jin, H., 2016. Antiviral activity of bictegravir (GS-9883), a novel potent HIV-1 integrase strand transfer inhibitor with an improved resistance profile. Antimicrob. Agents Chemother. 60, 7086–7097.

Zhang, X.-Y., Lu, W.-Y., 2014. Recent advances in lymphatic targeted drug delivery system for tumor metastasis. Cancer Biol. Med. 11, 247–254.